Mechanism of Heterogeneous Oxidation of Carbonyl Sulfide on Al_2O_3: An *in Situ* Diffuse Reflectance Infrared Fourier Transform Spectroscopy Investigation

Junfeng Liu, Yunbo Yu, Yujing Mu, and Hong He*

State Key Laboratory of Environmental Chemistry and Ecotoxicology, Research Center for Eco-Environmental Sciences, Chinese Academy of Sciences, Beijing 100085, China

Received: October 4, 2005; In Final Form: December 17, 2005

Heterogeneous reaction of carbonyl sulfide (OCS) on the surface of different types of alumina (Al_2O_3) at 298 K was investigated in a closed system and a flowed system using *in situ* diffuse reflectance infrared Fourier transform spectroscopy (DRIFTS). The effects of calcination temperature of the Al_2O_3 on its catalyzed reactivity were studied. The crystal structure and surface area of the Al_2O_3 were characterized using X-ray diffraction (XRD) and the Brunauer−Emmett−Teller (BET) method. This paper revealed that adsorbed OCS could be catalytically oxidized on the surface of Al_2O_3 to form *gas-phase* CO_2 and *surface* hydrogen carbonate (HCO_3^-) and sulfate (SO_4^{2-}) species at 298 K. The surface hydroxyl (OH) species on the Al_2O_3 had been found to be the key reactant for the heterogeneous oxidation of OCS. Furthermore, the *surface* hydrogen thiocarbonate ($HSCO_2^-$) species, an intermediate formed in the reaction of OCS with OH, can be observed on the thermal-treated Al_2O_3. On the basis of these results, the reaction mechanism of heterogeneous oxidation of OCS on Al_2O_3 *is* discussed.

1. Introduction

Carbonyl sulfide (OCS) is the most abundant atmospheric sulfur *containing* gas in the remote troposphere.[1,2] It is relatively inert in the troposphere, and it can be transported into the stratosphere where its *photooxidation* is considered to be an important source of stratospheric sulfate during volcanically quiescent periods.[1−5] From the point of view of the environment, it is important to study the global OCS cycle. Most studies focus on the homogeneous reaction of OCS with OH in the *gas-phase* and the consumption of OCS by the plants, soil, etc.[5] Heterogeneous interactions between gaseous molecules with wet or dry aerosol particles have gained considerable interest since they have the potential to alter the process of atmospheric chemistry significantly.[4,6] The surface of oxide particles in the atmosphere can adsorb and catalyze reactions of trace gases and, thus, change the chemical balance of the atmosphere.[7,8]

Aluminum is one of the most abundant elements *in atmospheric particles*. It has been reported that alumina (Al_2O_3) surface catalyzes the oxidation of H_2S or CS_2.[9,10] However, to our knowledge, very few studies have examined the possibility of heterogeneous reaction and the conversion pathway of OCS on the surface of atmospheric particles. Therefore, we studied the reaction mechanism of OCS on the surface of Al_2O_3 as a simplified model. To understand the mechanism of heterogeneous reaction of OCS on the Al_2O_3 surface, diffuse reflectance infrared Fourier transform spectroscopy (DRIFTS) was used in this study. DRIFTS can be used to observe the nature of the interaction of gas with a solid surface. In addition, *in situ* DRIFTS is especially useful to explore mechanisms of heterogeneous reactions of gases on a solid surface by providing information on reactive intermediates formed on the surface.

The present paper is devoted to a systematic *in situ* DRIFTS study on the mechanism of the heterogeneous reaction of OCS on the surfaces of four types of Al_2O_3. The surface hydrogen carbonate (HCO_3^-), *hydrogen thiocarbonate* ($HSCO_2^-$), and sulfate (SO_4^{2-}) species were found to be the major products formed from heterogeneous oxidation of OCS on the surface of Al_2O_3. *On the basis of* the experimental results, a composite reaction mechanism of heterogeneous oxidation of OCS on Al_2O_3 is proposed.

2. Experimental Section

2.1. Materials. Four types of Al_2O_3 used in this experiment were prepared from boehmite (AlOOH, Shandong aluminum Corporation) by calcining at different temperatures. The samples of Al_2O_3-A, Al_2O_3-B, Al_2O_3-C, and Al_2O_3-D were obtained by calcining AlOOH at 573, 873, 1273, and 1473 K for 3 h, respectively. Before DRIFTS measurement, all Al_2O_3 samples were pretreated in an *in situ* infrared cell by heating in 100 mL/min of O_2 at 873 K (except the Al_2O_3-A sample which was heated at 573 K) for 3 h.

All reactant gases were used without further purification as follows: *Carbonyl sulfide* (OCS, 2%, OCS/N_2, Scott Specialty Gases Inc.); O_2 (99.99% purity, Beijing AP BEIFEN Gases Inc.).

2.2. Techniques of Characterization. *BET Experiment.* The nitrogen adsorption−desorption isotherms were obtained at 77 K over the whole range of relative pressures, using a Micromeritics ASAP 2000 automatic equipment. Specific areas were computed from these isotherms by applying the Brunauer−Emmett−Teller (BET) method.

X-ray Diffraction Experiment. The samples were characterized by X-ray diffractometry using a computerized Rigaku D/max-RB diffractometer (Japan, Cu Ka radiation, 1.54056 nm). The step scans were taken over a 2θ range of 10−90° in steps of 0.02°/s.

In Situ DRIFTS Experiment. In Situ DRIFTS spectra were recorded on a NEXUS 670 (Thermo Nicolet Instrument Corporation) FT-IR, equipped with an *in situ* diffuse reflection

* Corresponding author. Phone: +86-10-62849123. Fax: +86-10-62849123. E-mail: honghe@ rcees.ac.cn.

10.1021/jp055646y CCC: $33.50
Published on Web 02/02/2006

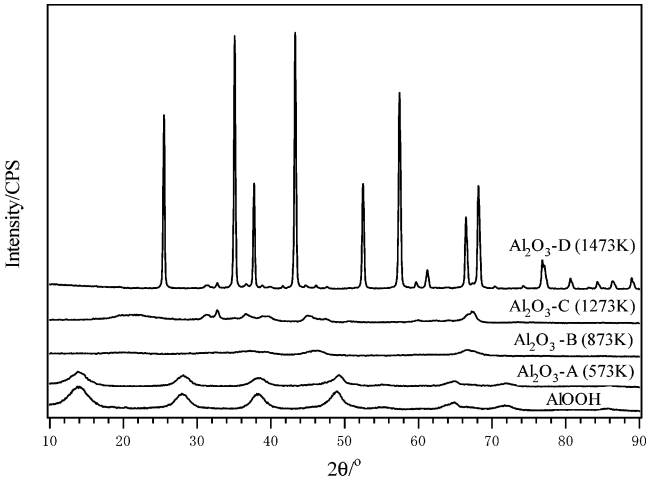

Figure 1. X-ray diffraction patterns of Al_2O_3 samples.

TABLE 1: Specific Area of the Al_2O_3 and AlOOH Samples

sample	AlOOH	Al_2O_3-A	Al_2O_3-B	Al_2O_3-C	Al_2O_3-D
BET area (m^2/g)	318	277	257	121	12

chamber and a high-sensitivity mercury cadium telluride (MCT) detector cooled by liquid N_2. The sample *(about 11 mg)* for the *in situ* DRIFTS studies was finely ground and placed into a ceramic crucible in the *in situ* chamber. *The total flow rate was 100 mL/min in all the flow systems, and the volume of the closed system was 30 mL*. The reference spectrum was measured after the *pretreated* sample was cooled to 298 K in a purified O_2 stream. The infrared spectra were collected and analyzed using a data acquisition computer with OMNIC 6.0 software (Nicolet Corp.) installed. All spectra reported here were recorded at a resolution of 4 cm^{-1} for 100 scans.

2.3. Calibration Curve of the Gas-Phase OCS Concentration. A series of *in situ* DRIFTS spectra at a steady state of the flow system with various concentrations of OCS (40−2000 ppm) were recorded at 298 K. The integrated areas of the absorption peak of gaseous OCS in the range of 1980−2120 cm^{-1} have a linear correlation with the concentration of OCS gas ($R^2 > 0.99$). The concentration of *gas-phase* OCS was determined by measuring the *in situ* DRIFTS spectra peak areas of gaseous OCS.

3. Results and Discussion

3.1. Characterizations. *BET.* BET results are shown in Table 1. The surface areas of the AlOOH, Al_2O_3-A, Al_2O_3-B, Al_2O_3-C, and Al_2O_3-D samples were decreasing with the increasing calcination temperature.

X-ray Diffraction. The XRD patterns of all samples of *AlOOH and AlOOH* calcined at 573, 873, 1273, and 1473 K are presented in Figure 1. The Al_2O_3-A sample shows a characteristic of an amorphous structure and still exists mainly as AlOOH. Signals due to the γ-Al_2O_3 ($2\theta = 67°$, 46°, and 37°) can be seen in the type Al_2O_3-B sample.[11] The Al_2O_3-C sample exists mainly as the crystal of θ-Al_2O_3, and the crystal of γ-Al_2O_3 is also observed in Al_2O_3-C.[12,13] The Al_2O_3-D sample exists mainly as the crystal of α-Al_2O_3 evidence in line at $2\theta = 43°$, 35°, and 57°.[12,13] With rising of the calcination temperature, the crystal structure of Al_2O_3 changes from γ-Al_2O_3 to θ-Al_2O_3 and then to α-Al_2O_3.[14]

3.2. Heterogeneous Reaction of OCS on the Al_2O_3 samples in a Closed System. The Al_2O_3-A sample (AlOOH calclined at 573 K for 3 h) was exposed to a flow of 1000 ppm OCS + 95% O_2 at 298 K for 5 min, and then, the inlet and outlet were closed. The *in situ* DRIFTS spectra on the Al_2O_3-A sample were recorded as a function of time and are shown in Figure 2. Strong peaks of *gas-phase* OCS appeared at 2071 and 2052 cm^{-1}.[15,16] A pair of peaks of gaseous carbon dioxide (CO_2) was observed at 2337 and 2361 cm^{-1}.[17,18] *The* bands at 1647 and 1412 cm^{-1} are due to ν_{as}(OCO) and ν_s(OCO) of *surface HCO_3^- species*, respectively,[15,17−19] and *the* very weak band at 1354 cm^{-1} is assigned to surface SO_4^{2-} species.[20−24] *It is also found that the peaks for gas-phase CO_2 and surface SO_4^{2-} species increased in intensity with time, while the peaks of gaseous OCS diminished. The bands for HCO_3^- were not grown apparently from 2 to 20 min, because the surface HCO_3^- species is the intermediate of OCS oxidation, and exist in a dynamic balance process of formation and consumption. These results suggest that OCS in O_2 can be finally converted into gas-phase CO_2 and surface SO_4^{2-} species on the Al_2O_3-A sample surface at 298 K.*

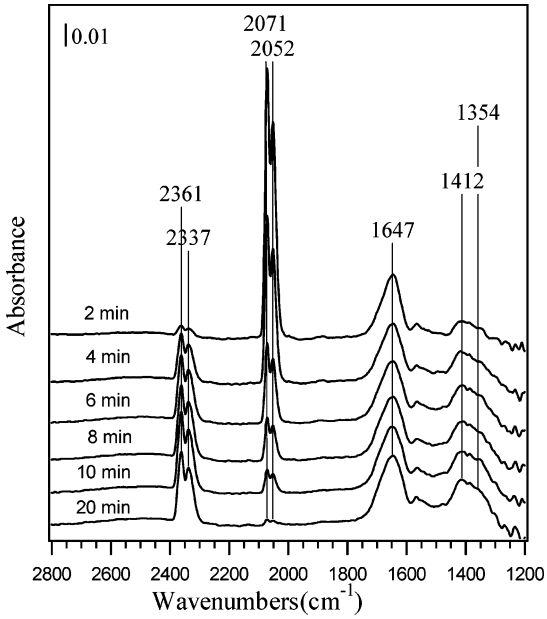

Figure 2. Dynamic changes of *in situ* DRIFTS spectra of the Al_2O_3-A sample as a function of time after exposure to 1000 ppm OCS + 95% O_2 in a closed system at 298 K.

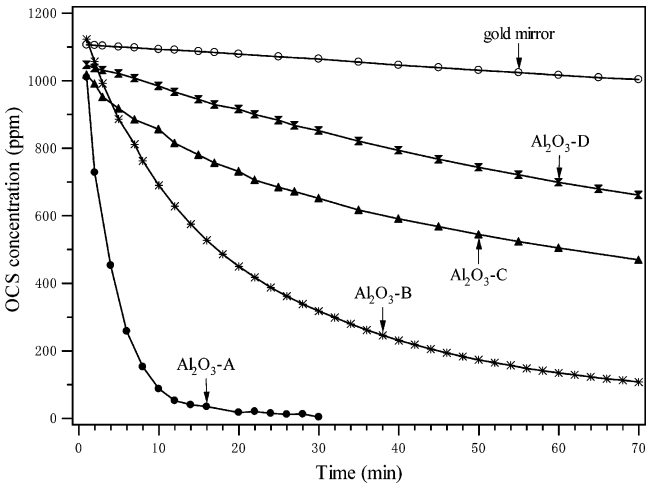

Figure 3. Heterogeneous reaction of 1000 ppm OCS + 95% O_2 on the Al_2O_3-A, Al_2O_3-B, Al_2O_3-C, and Al_2O_3-D samples or a gold mirror at 298 K in a closed system.

The same set experiments were also carried out using the Al_2O_3-B (γ-Al_2O_3), Al_2O_3-C (θ-Al_2O_3), and Al_2O_3-D (α-Al_2O_3) samples, respectively. The *gas-phase* OCS concentrations shown

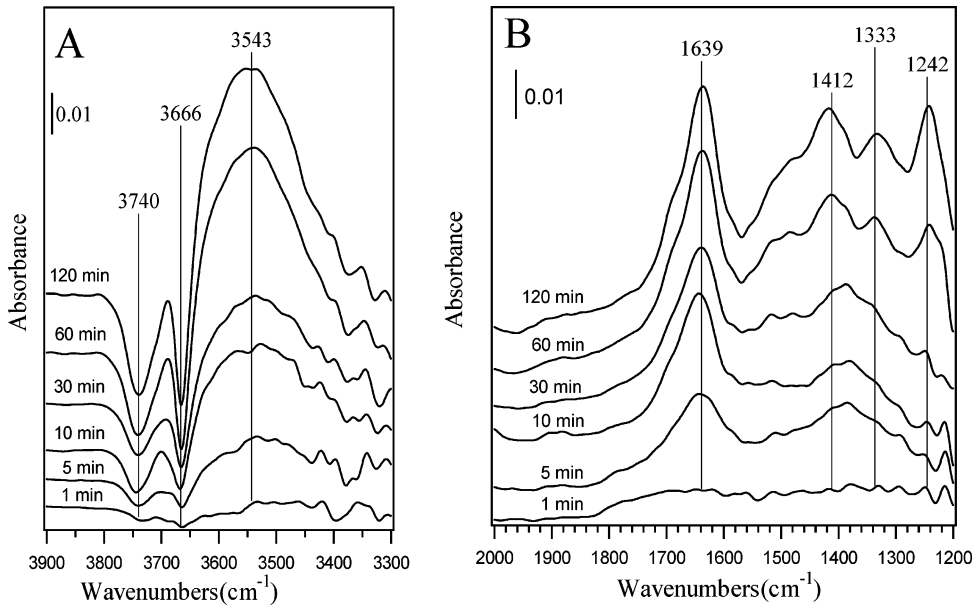

Figure 4. Dynamic changes of *in situ* DRIFTS spectra of the Al_2O_3-A sample as a function of time in a flow of 1000 ppm OCS + 95% O_2 at 298 K.

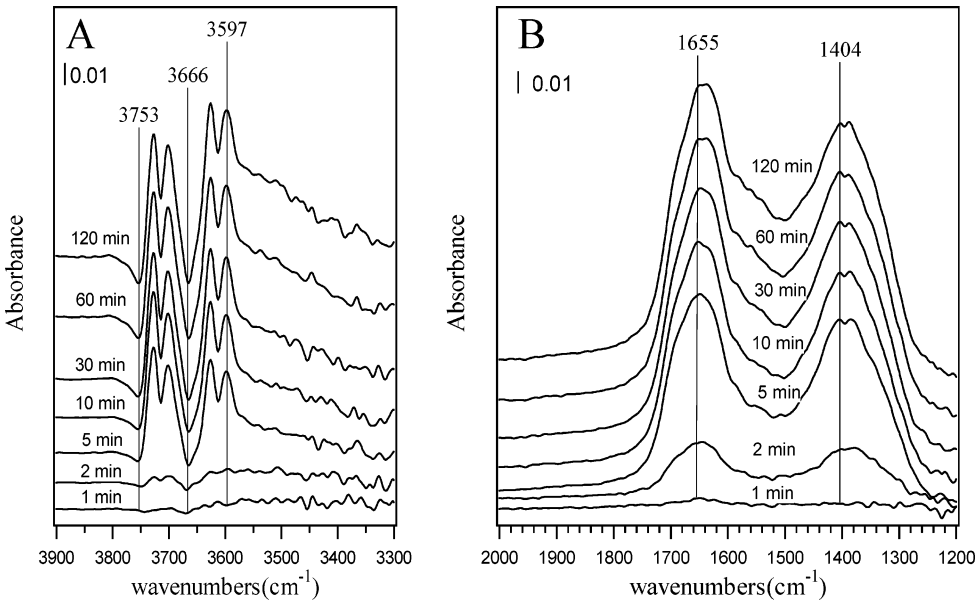

Figure 5. Dynamic changes of *in situ* DRIFTS spectra of the Al_2O_3-A sample as a function of time in a flow of 1000 ppm CO_2 + 95% O_2 at 298 K.

in Figure 3 were determined by comparing the OCS absorbance peak area with the calibration curve of the *gas-phase* OCS concentration. To distinguish the effect of the surface of the system on the loss of OCS, a control experiment was performed under the same conditions by replacing Al_2O_3 sample with a gold mirror. In this case, only a very weak change of the *gas-phase* OCS concentration was observed during the experiment, indicating that the system may consume a small quantity of OCS through the adsorption or the heterogeneous reaction catalyzed by the surface of the system. The concentration of gaseous OCS drastically decreases with the Al_2O_3-A sample, whereas it decreases mildly with the Al_2O_3-B, Al_2O_3-C, and Al_2O_3-D samples. It is thought that the surface area has an important influence on the absorption and reaction of OCS; however, the Al_2O_3-A and Al_2O_3-B samples have similar surface areas, but they exhibit different reaction rates. Therefore, there must be other factor affecting the decrease of OCS.

3.3. Dynamic State *in Situ* DRIFTS Study of OCS + 95% O_2 on the Al_2O_3-A Samples in a Flow System. To gain further information about the reaction of OCS on the Al_2O_3-A sample, *in situ* DRIFTS spectra of the Al_2O_3-A sample as a function of time were measured in a flow of 1000 ppm OCS + 95% O_2 at 298 K (Figure 4). Similar to Figure 2, the peaks due to surface HCO_3^- (1639 and 1412 cm^{-1}) and SO_4^{2-} (1333 cm^{-1}) were observed, and the intensities of these peaks increased with time during 120 min (Figure 4B). *On the basis of* the previous studies, the peak located at 1242 cm^{-1} could be assigned as the vibration of *surface HCO_3^- species*[15,17−19] or be assigned to *surface HSO_3^- species*.[25,26] To confirm our assignments about the surface HCO_3^- and HSO_3^- species, the Al_2O_3-A sample was exposed to a flow of 1000 ppm CO_2 + 95% O_2 at 298 K. As can be seen in Figure 5B, the vibration peaks of *surface HCO_3^- species* were located at 1655 and 1404 cm^{-1} on the Al_2O_3-A sample. While the Al_2O_3-A sample was exposed to a flow of

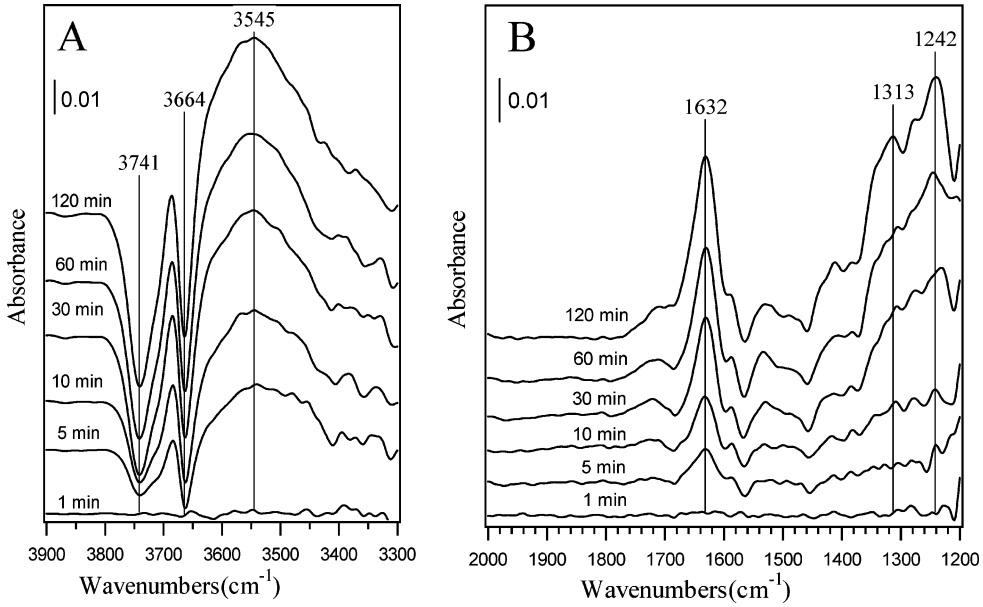

Figure 6. Dynamic changes of *in situ* DRIFTS spectra of the Al_2O_3-A sample as a function of time in a flow of 200 ppm SO_2 + 95% O_2 at 298 K.

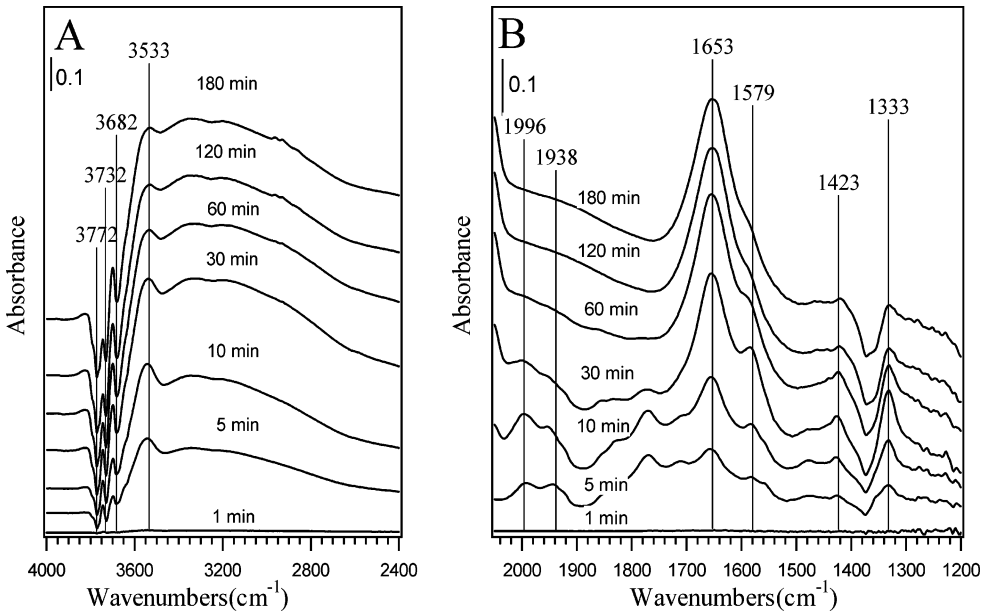

Figure 7. Dynamic changes of *in situ* DRIFTS spectra of the Al_2O_3-B ($\gamma-Al_2O_3$) sample as a function of time in a flow of 1000 ppm OCS + 95% O_2 at 298 K.

200 ppm SO_2 + 95% O_2 at 298 K, as shown in Figure 6B, the vibration peaks of *surface HSO_3^- species* were located at 1242 cm^{-1}. Therefore, we finally assigned the peak located at 1242 cm^{-1} (in Figure 4B) to the vibration mode of *surface HSO_3^- species* instead of *surface HCO_3^- species*. The broad band centered at 3543 cm^{-1} was assigned to the ν(OH) stretching of adsorbed H_2O.[13,27] The peak at 1639 cm^{-1} was assigned to a combination band produced from ν_{as}(OCO) of surface HCO_3^- species and δ(HOH) of adsorbed H_2O, and the peak at 1412 cm^{-1} was assigned to ν_s(OCO) of surface HCO_3^- species.[15,17−19]

Meanwhile, it should be noted that introduction of 1000 ppm OCS led to a drastic increase in the intensity of negative peaks at 3740 and 3666 cm^{-1} in Figure 4A. In the model proposed by Peri,[28,29] these bands were attributed to the vibrations of surface hydroxyl (OH) species. The consumption of surface OH species meant that the reaction between OCS and surface OH must occur. However, other intermediates, favorable for understanding the mechanism of OCS conversion, were not measured in this rapid reaction. Considering *that* the thermal pretreatment of Al_2O_3 was expected to reduce the surface OH groups, further experiments were performed on the thermal pretreatment of Al_2O_3 samples to observe these intermediates.

Figure 7 shows the *in situ* DRIFTS spectra of the Al_2O_3-B sample in a flow of OCS + 95% O_2 at 298 K. The bands at 1653 and 1423 cm^{-1} provided similar evidence for the formation of surface HCO_3^- species, but the intensity ratio of 1653 and 1423 cm^{-1} indicates a low surface concentration of HCO_3^- species and a lot of adsorbed H_2O. It should be noted that a new peak at 1579 cm^{-1} was observed, which is assignable to *surface hydrogen thiocarbonate ($HSCO_2^-$) species* as an intermediate of the hydrolysis of OCS.[15,30,31] Meanwhile, the peaks located at 1996 and 1938 cm^{-1} due to the physically adsorbed OCS were observed at the beginning of the reaction and then diminished.[30,31] *This diminishing of the physically adsorbed OCS may be derived from the competition adsorption*

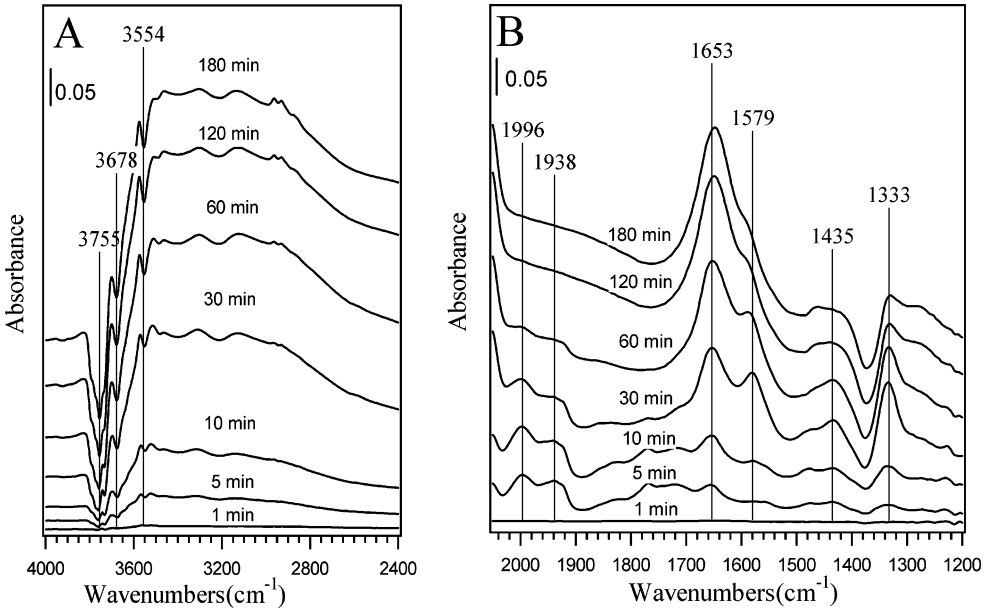

Figure 8. Dynamic changes of *in situ* DRIFTS spectra of the Al_2O_3-C sample as a function of time in a flow of 1000 ppm OCS + 95% O_2 at 298 K.

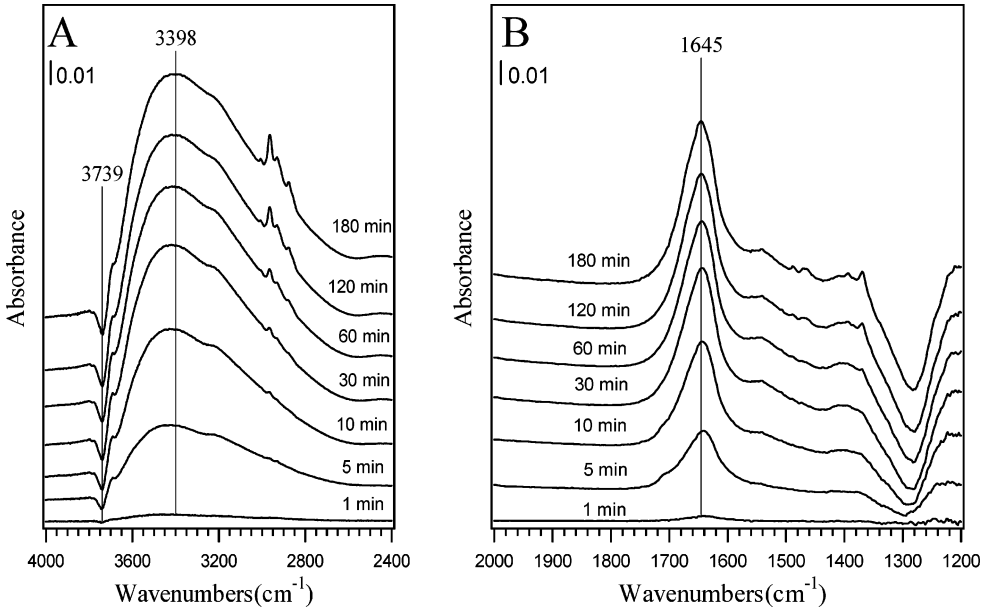

Figure 9. Dynamic changes of *in situ* DRIFTS spectra of the Al_2O_3-D sample as a function of time in a flow of 1000 ppm OCS + 95% O_2 at 298 K.

between the chemically adsorbed surface species (e.g. HCO_3^-) and the physically adsorbed OCS.

It *is* apparent that the thermal treatment of Al_2O_3 could slow OCS oxidation and enable the observation of the reaction intermediate. In the region of OH groups, a drastic increase in the intensity of negative peaks at 3772, 3732, and 3682 cm^{-1} attributed to the vibrations of surface OH groups (Figure 7A) was observed. These results strongly suggest that the formation of surface $HSCO_2^-$ species is derived from the reaction between surface OH species and OCS. Although the thermal treatment of Al_2O_3 could reduce the surface OH species and the formation of surface $HSCO_2^-$ species, the conversion rate of *surface $HSCO_2^-$ species* into surface HSO_3^- species under this condition might be decreased more greatly; thus, *surface $HSCO_2^-$ species* were clearly detected. This indicates that the surface OH species play an important role in the formation of *surface $HSCO_2^-$ species* and that the *surface $HSCO_2^-$ species* converted into *surface* HSO_3^- and HCO_3^- species also need the participation of the surface OH species.

To confirm the presence of *surface $HSCO_2^-$ species* as an intermediate of OCS oxidation, the same experiment was performed on the Al_2O_3-C sample (AlOOH calclined at 1273 K for 3 h). As shown in Figure 8, exposure of the sample to OCS resulted in the appearance of *surface* HCO_3^- (1653 and 1435 cm^{-1}), $HSCO_2^-$ (1579 cm^{-1}), and SO_4^{2-} species (1333 cm^{-1}) (Figure 8B), which was also accompanied by the formation of negative peaks at 3755 and 3678 cm^{-1} due to surface OH groups (Figure 8A). Obviously, the oxidation of OCS shows the same mechanism on the Al_2O_3-B and Al_2O_3-C samples. However, high-temperature calcination of AlOOH resulted in an activity loss of catalytic oxidation for OCS, as evidenced by the lower reaction rate (Figure 3).

To further investigate the role of surface OH groups in OCS oxidation on Al_2O_3, the same experiment was performed on the

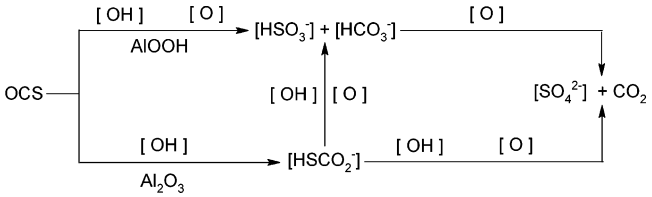

Figure 10. Mechanism of heterogeneous oxidation of OCS on the AlOOH and Al_2O_3 samples.

Al_2O_3-D sample on which surface OH groups were absent in comparison with the γ-Al_2O_3 sample. As shown in Figure 9A, a small quantity of negative peaks due to OH groups (3739 cm^{-1}) was detected, and no peaks attributable to *surface* $HSCO_2^-$, HCO_3^-, and SO_4^{2-} species were observed (Figure 9B). In addition, the peak due to surface adsorbed H_2O (3398 and 1645 cm^{-1}) was detected. This result confirms our suggestion about the role of *surface* OH groups in OCS oxidation on the γ-Al_2O_3 surface.

3.4. Proposed Mechanism of Heterogeneous Oxidation of OCS on Al_2O_3. *On the basis of* the above results, we propose the following possible mechanism of the heterogeneous oxidation of OCS on Al_2O_3, as shown in Figure 10.

OCS first reacted with the surface OH species to form the surface $HSCO_2^-$ species on AlOOH and γ-Al_2O_3 at room temperature. The oxidation of *surface* $HSCO_2^-$ *species* by *oxygen containing surface species* and the surface OH species proceeded readily, followed by the formation of the surface HCO_3^- and SO_4^{2-} species at room temperature. When the *oxygen containing surface species* were consumed, O_2 in the *gas-phase* can supplement it so that the oxidation reaction can continue until the surface is fully covered by *surface* HCO_3^- and SO_4^{2-} species. Both the *oxygen containing surface species and surface* OH species can contribute to this reaction. When the heat-treated Al_2O_3 samples were exposed to OCS + 95% O_2, the reaction between surface OH with *surface* $HSCO_2^-$ *species* was slowed. At the same time, the conversion rate of *surface* $HSCO_2^-$ *species* into surface HSO_3^- species under this condition might be decreased more greatly. As a result, surface $HSCO_2^-$ species became the dominant surface species. This enables the observation of the reaction intermediate during the heterogeneous oxidation of OCS over Al_2O_3.

4. Conclusions

This study reveals that OCS can be catalytically oxidized on Al_2O_3 surface to produce *gas-phase* CO_2 and surface SO_4^{2-} species as final products at 298 K. *Surface* $HSCO_2^-$ *species* were found to be an important intermediate formed by the reaction of OCS with surface OH species. *Surface* HSO_3^- and HCO_3^- species were also found as reaction intermediates subsequently. The thermal treatment of Al_2O_3 apparently slowed the heterogeneous oxidation of OCS through reducing the surface OH species, which is implied as the key reactant of the reaction.

Acknowledgment. This research was financially supported by the National Natural Science Foundation of China (40275038).

References and Notes

(1) Crutzen, P. J. *Geophys. Res. Lett.* **1976**, *3*, 73−76.
(2) Torres, A. L.; Maroulis, P. J.; Goldberg, A. B.; Bandy, A. R. *J. Geophys. Res.* **1980**, *85*, 7357−7360.
(3) Turco, R. P.; Whitten, R. C.; Toon, O. B.; Pollack, J. B.; Hamill, P. *Nature* **1980**, *283*, 283−286.
(4) Andreae, M. O.; Crutzen, P. J. *Science* **1997**, *276*, 1052−1058.
(5) Watts, S. F. *Atmos. Environ.* **2000**, *34*, 761−779.
(6) Baltensperger, U.; Ammann, M.; Kalberer, M.; Gäggeler, H. W. *J. Aerosol Sci.* **1996**, *27*, S651−S652.
(7) Ravishankara, A. R. *Science* **1997**, *276*, 1058−1065.
(8) Al-Abadleh, H. A.; Grassian, V. H. *Surf. Sci. Rep.* **2003**, *52*, 63−161.
(9) Datta, A.; Cavell, R. G. *J. Phys. Chem.* **1985**, *89*, 450−454.
(10) Wang, L.; Zhang, F.; Chen, J. *Environ. Sci. Technol.* **2001**, *35*, 2543−2547.
(11) Aytam, H. P.; Akula, V.; Janmanchi, K.; Kamaraju, S. R. R.; Panja, K. R.; Gurram, K.; Niemantsverdriet, J. W. *J. Phys. Chem. B* **2002**, *106*, 1024−1031.
(12) Lu, H.; Sun, H.; Mao, A.; Yang, H.; Wang, H.; Hu, X. *Mater. Sci. Eng., A* **2005**, *406*, 19−23.
(13) Bhattacharya, I. N.; Gochhayat, P. K.; Mukherjee, P. S.; Paul, S.; Mitra, P. K. *Mater. Chem. Phys.* **2004**, *88*, 32−40.
(14) Morterra, C.; Magnacca, G. *Catal. Today* **1996**, *27*, 497−532.
(15) Lavalley, J. C.; Travert, J.; Chevreau, T.; Lamotte, J.; Saur, O. *J. Chem. Soc., Chem. Commun.* **1979**, *4*, 146−148.
(16) Zittel, P. F.; Sedam, M. A. *J. Phys. Chem.* **1990**, *94*, 5801−5809.
(17) Amenomiya, Y.; Morikawa, Y.; Pleizier, G. *J. Catal.* **1977**, *46*, 431−433.
(18) Morterra, C.; Zecchina, A.; Coluccia, S.; Chiorino, A. *J. Chem. Soc., Faraday Trans.* **1977**, *73*, 1544−1560.
(19) Molina, R.; Centeno, M. A.; Poncelet, G. *J. Phys. Chem. B* **1999**, *103*, 6036−6046.
(20) Saur, O.; Bensitel, M.; Mohammed Saad, A. B.; Lavalley, J. C.; Tripp, C. P.; Morrow, B. A. *J. Catal.* **1986**, *99*, 104−110.
(21) Lavalley, J. C. *Catal. Today* **1996**, *27*, 377−401.
(22) Meunier, F. C.; Ross, J. R. H. *Appl. Catal., B* **2000**, *24*, 23−32.
(23) Sahibed-Dine, A.; Aboulayt, A.; Bensitel, M.; Mohammed Saad, A. B.; Daturi, M.; Lavalley, J. C. *J. Mol. Catal. A: Chem.* **2000**, *162*, 125−134.
(24) Yang, Q.; Xie, C.; Xu, Z.; Gao, Z.; Du, Y. *J. Phys. Chem. B* **2005**, *109*, 5554−5560.
(25) Laniecki, M.; Ziólek, M.; Karge, H. G. *J. Phys. Chem.* **1987**, *91*, 4−6.
(26) Mitchell, M. B.; Sheinker, V. N.; White, M. G. *J. Phys. Chem.* **1996**, *100*, 7550−7557.
(27) Goodman, A. L.; Bernard, E. T.; Grassian, V. H. *J. Phys. Chem. A* **2001**, *105*, 6443−6457.
(28) Peri, J. B.; Hannan, R. B. *J. Phys. Chem.* **1960**, *64*, 1526−1530.
(29) Peri, J. B. *J. Phys. Chem.* **1965**, *69*, 220−230.
(30) Lavalley, J. C.; Aboulayt, K.; Lion, M.; Bachelier, J.; Hebrard, J. L.; Luck, F. *Proceedings of the American Chemical Society Atlanta meeting*, April 14−19, 1991; 43−49.
(31) Hoggan, P. E.; Aboulayt, A.; Pieplu, A.; Nortier, P.; Lavalley, J. C. *J. Catal.* **1994**, *149*, 300−306.